Influence of Size Effect on Dynamic Mechanical Properties of OFHC Copper at Micro/Mesoscopic Scale

Chuanzhi Jing
Shandong University
Jilai Wang (jlwang@sdu.edu.cn)
Shandong University https://orcid.org/0000-0002-1010-5573
Chengpeng Zhang
Shandong University
Yan Sun
Shandong Nonmetallic Materials Institute
Zhenyu Shi
Shandong University

Research Article

Keywords: Dynamic mechanical properties, High strain rate, Surface layer model, J-C model, Micro/meso-scale

Posted Date: August 30th, 2021

DOI: https://doi.org/10.21203/rs.3.rs-822494/v1

Influence of size effect on dynamic mechanical properties of OFHC copper at micro/mesoscopic scale

Chuanzhi Jing[a,b], Jilai Wang[a,b*], Chengpeng Zhang[a,d], Yan Sun[c], Zhenyu Shi[a,b**]

[a] Key Laboratory of High Efficiency and Clean Mechanical Manufacture of Ministry of Education, School of Mechanical Engineering, Shandong University, Jinan, Shandong, 250061, China

[b] National Demonstration Center for Experimental Mechanical Engineering Education, Shandong University, Jinan, Shandong, 250061, China

[c] Shandong Nonmetallic Materials Institute, Jinan, Shandong, 250031, China

[d] State Key Laboratory of Mechanical System and Vibration, Shanghai Jiao Tong University, Shanghai 200240, China

Abstract

The dynamic mechanical properties of metallic materials have been extensively investigated at the macro-scale in terms of deformation mechanisms, strain rate strengthening, and fracture mechanisms. However, the dynamic mechanical properties affected by size effects at micro/meso-scales have rarely been investigated. To explore the size effects on the dynamic mechanical properties at micro/meso-scales, the experiments of quasi-static compression and SHPB were carried out using oxygen-free, high-conductivity (OFHC) copper with different geometrical and grain sizes. The experimental results show that the quasi-static and dynamic mechanical properties of OFHC copper are affected by size effects at micro/meso-scales. In particular, OFHC copper exhibits strain rate strengthening effects at the micro/meso-scales, and the presence of micro-cracks was observed in the SHPB experimental specimens. The J-C constitutive model based on the surface layer model is proposed and the analysis of the average relative error of the modified model and the original constitutive model is performed. Finite element analysis was carried out based on the modified J-C model and the original model, and the results show that the

Corresponding author: Jilai Wang*
Email: jlwang@sdu.edu.cn

modified J-C model was in good agreement with the experimental results.

Keywords: Dynamic mechanical properties, High strain rate, Surface layer model, J-C model, Micro/meso-scale

1.Introduction

With the rapid development of miniaturization products and micro electro mechanical systems (MEMS), the trend of miniaturization of products is increasing, and micro components are widely used in microelectronics, medical, automotive, and aerospace industries [1-3]. The study of the dynamic mechanical properties of micro parts at the micro/meso-scales is important for military demolition, high speed cutting and stamping. However, the emergence of size effects, namely, grain size and geometrical size effects, greatly influence the mechanical properties of metallic materials.

The influence of size effects on the strength and formability of metallic alloy components was reviewed [4, 5]. Jiang et al. [6] conducted dynamic shear tests using the hat-shaped samples with different shear ring thicknesses and the results showed that the shear stress and fracture strain increased as the shear ring thickness decreased. Zhang et al. [7] found that the mechanical properties of the 7075-T6 aluminum alloy were influenced by the strain rate and showed a significant strain rate hardening effect. Tanner et al. [8] have studied strain rate and temperature history effects on Oxygen-free high-conductivity (OFHC) copper. Work done by Smerd et al. [9] shown that Al-Mg alloys AA5754 and AA5182 exhibited low strain rate sensitivity at both room and high temperatures. The dynamic mechanical properties of selective laser melted Ti-6Al-4V alloy exhibits an increase in yield stress with increasing strain rate, showing a significant strain rate sensitivity. This phenomenon can be explained as an increase in plasticity induced by the strain rate effect [10]. Mechanical experiments on different metal and alloy materials at high strain rates were conduted to study the mechanical properties of the materials under dynamic loading and the deformation mechanism [11-14].

The constitutive model is usually used to describe the functional relationship among strain, strain rate, and temperature in plastic deformation of materials.The constitutive model of metal under a high strain rate can be divided into two kinds [15]. One is the

empirical constitutive model, including Johnson-Cook (J-C) constitutive model [16], Khan–Huang (KH) model [17], and some other empirical models [18-20]. The other one is the physically based constitutive model, including Zerilli-Armstrong (Z-A) constitutive model [21], Mechanical Threshold Stress (MTS) constitutive model [22], and NN-Li constitutive model [23]. The characteristic of empirical equations is that stress can be expressed as functions of strain, strain rate, and temperature and their parameters can be easily obtained from experimental data. Physically based constitutive model can reflect the micro-scale changes of material during the deformation process such as dislocation, thermal activation, and recrystallization. Huh et al. [24] evaluated the applicability of six constitutive models of FCC, BCC, HCP metals, including Johnson-Cook (J-C), Zerrilli-Armstrong, Preston-Tonks-Wallace, Modified Johnson-Cook, and Modified Khan-Huang models. Among the models, J-C model is the most commonly used constitutive model under the high strain rate. This model takes into account the influence of strain hardening, strain rate strengthening, and thermalsoftening phenomenon, moreover, have simple form and few parameters, which can easily be obtained by experiments.

H. K. et al. [25] determined the parametersof the J-C model for Inconel 718 by quasi-static tensile tests, flat plate impinging on a steel ball and simulation using ABAQUS. Ducobu et al. [26] gathered twenty sets of J-C parameters for Ti-6Al-4V and put into a Coupled Eulerian-Lagrangian (CEL) finite element orthogonal cutting model. Then an accurate method for cutting were obtained by comparing all numerical simulations with experimental results in the same condition. However, the original model is not universal. J-C model was modified in many researches. Zhang et al. [7] modified the strain rate hardening term of the J-C model through experimental data, which was more accurate than the original J-C model. Gambirasio et al. [27] introduced a modified J-C model, namely Split Johnson-Cook model, and this model solved the problem that the equivalent plastic strain rate and temperature have different effects on each equivalent plastic strain. However, the dynamic mechanical

properties of materials at micro/mesoscopic scales have rarely been studied. Moreover, the original and the modified J-C models are mostly applied to the prediction of the dynamic properties of materials at macro-scale, and the size effects are rarely taken into account in the model for modification and application to the dynamic mechanical properties at micro/meso-scales.

In this study, OFHC copper of different geometrical sizes with different grain sizes were used to investigate the influence of size effects on dynamic mechanical properties. The specimens were subjected to quasi-static and split Hopkinson press bar tests at micro/meso-scales. The metallographic and microstructure of the specimens after the experiments were observed to investigate the deformation mechanism at the micro/meso-scales. A modified J-C model based on the surface layer model was proposed to study the size effects. The parameters were fitted using experimental data from quasi-static and separated Hopkinson pressbar tests, and the proposed model was verified through the experiments.

2. Experiments

2.1 Workpiece materials

The commercially oxygen-free high-conductivity (OFHC) copper was chosen as the experimental material, which was widely used in the electronic and optical components. The shape of the specimen is cylindrical with a height to diameter ratio of 1:1. The diameter of the specimen is 0.5, 1, and 2 mm. The 1mm specimens were annealed at 450 °C for 2h, 600 °C for 2h, and 750 °C for 3h to obtain different grain sizes and to study the effect of grain size on the mechanical properties of OFHC copper at the micro/meso-scales. Heat treatment conditions as shown in Table 1. The heat-treated specimens were grinded, polished, and etched to obtain the metallographic microstructure, as shown in Fig. 1.

Table 1 Annealing treatment parameters and grain size

	Annealed temperature	Dwelling time	Average grain size (Standard deviation)
Group 1	450 ℃	2h	30 um(3.6)
Group 2	600 ℃	2h	40 um(5.2)
Group 3	750 ℃	3h	50 um(6.5)

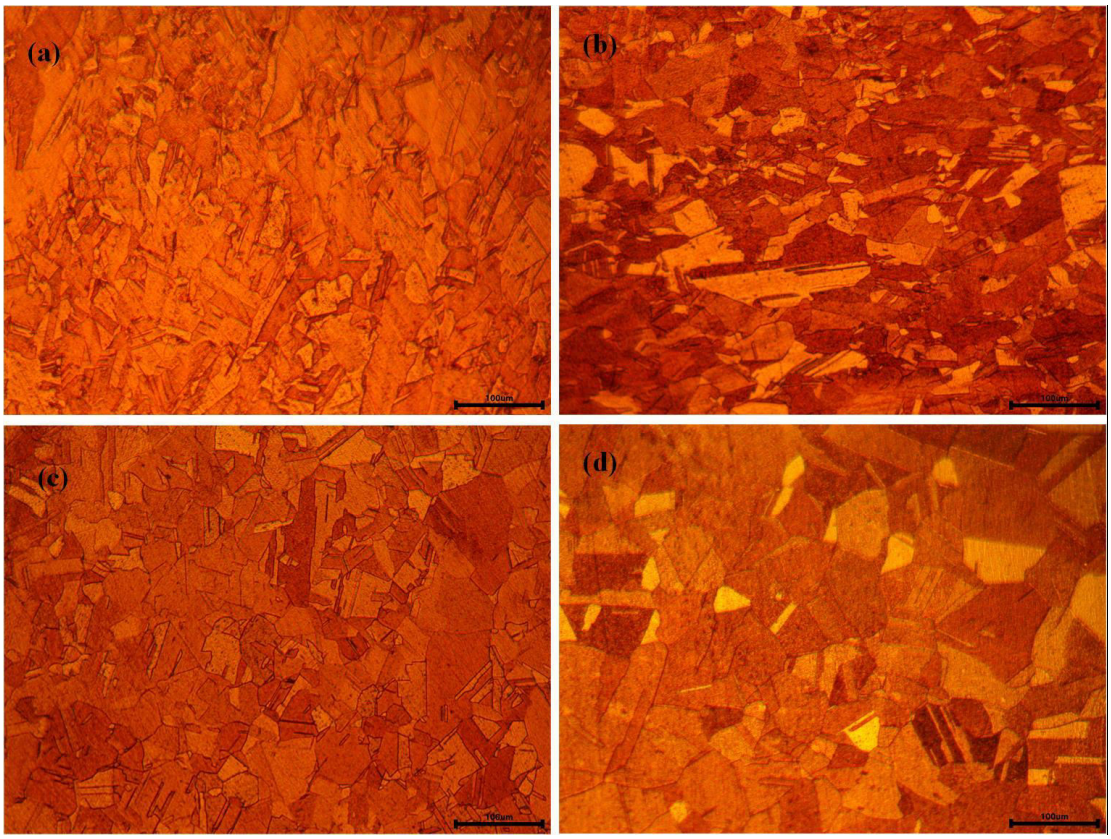

Fig. 1. Microstructure of annealed OFHC copper. (a) as-received , (b) 450 ℃ , (c) 600 ℃ , and (d) 750 ℃ .

2.2 Experimental setup

The quasi-static mechanical properties of the specimens were obtained by compression tests on a universal testing machine with a pressure transducer of 5 kN. In order to ensure the accuracy of the experiment, a stamping fixture with low surface roughness values and high flatness were designed. Lubricants were also applied to the ends of the specimens to further reduce the effects of friction. Each set of experiments was performed three times to eliminate experimental chance errors. Firstly, the quasi-static compression tests were carried out on specimens of different grain sizes to

investigate the grain size effect on the quasi-static mechanical properties of OFHC copper. Quasi-static compression tests were then carried out on different feature sizes to investigate the geometrical size effect on the quasi-static mechanical properties of OFHC copper. Compression tests were also carried out on 1mm specimens at 30%, 40%, 50% and 70% downward displacement to investigate the plastic deformation process of the specimens, and additional compression tests at 50% downward displacement were carried out on 0.5mm and 2mm to investigate the effect of size effect on the mechanical properties.

The dynamic mechanical properties of the specimen were obtained by using a split Hopkinson press bar device (SHPB). The impact bar of tests was blown through the gas in the storage chamber, and the air pressure is vaired in the chamber for different strain rate experiments. The ends of the specimen are applied grease to reduce the effects of friction. The analysis of the one-dimensional stress waves generated by the incident and projected rods utilizing a hyper-dynamic data acquisition system to obtain the dynamic stress-strain curves of the specimen. SHPB tests were performed at strain rates of 7000, 9000, and 13000 s^{-1} to investigate the grain size effect on the dynamic mechanical properties of OFHC copper. The 0.5 and 2mm specimens were also annealed at a temperature of 600 °C for 2h, followed by SHPB tests to investigate the grometrical size effect on the mechanical properties.

3. Results and analysis

3.1 The results and analysis of quasi-static compression experiments

Fig. 2 shown that the true stress-strain curves of the four different grain sizes were all work-hardened and had similar trends under quasi-static compression. As the heat treatment temperature increases and the holding time grows, the flow stress decrease with the increase of grain size. This phenomenon has been associated with peer researches [3, 28]. The reason for this is that when the geometrical size is the same, the increasing in grain size increases the ratio of surface grains to all grains, which

makes it easier to torsion and deformation as the surface grains are less constrained.The original specimen without heat treatment was influenced by the previous machining process, and had the highest flow stress. Due to frictional effects the true stress-strain curves of the 600 °C annealed specimens are very close to those of the 750 °C annealed specimens. From Fig.3, it can be seen that the reduction in flow stress of the material decreases with decreasing geometric size for the same grain size, which is consistent with Chan's research [29], and shows the phenomenon: "the smaller, the weaker". When the grain size is the same, the smaller geometrical size leads to an increase in the number of surface grains. In the plastic deformation process, the surface grain is more prone to plastic deformation and the flow stress of the material is reduced.

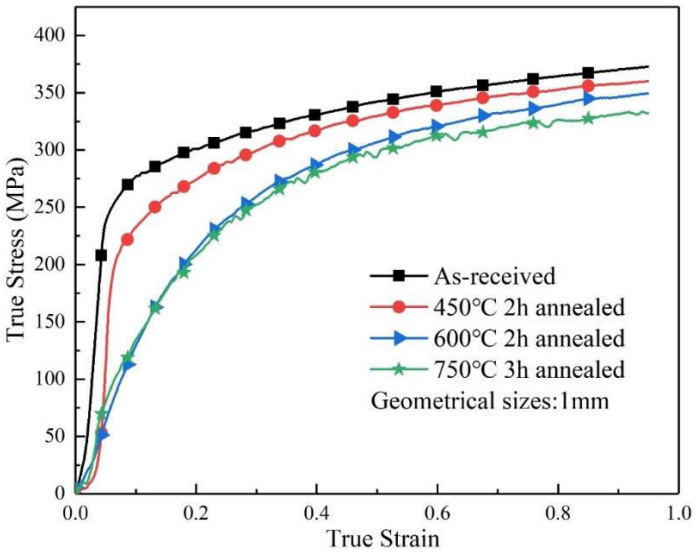

Fig.2. The true stress-strain curves of quasi-static compression for specimens with different grain sizes.

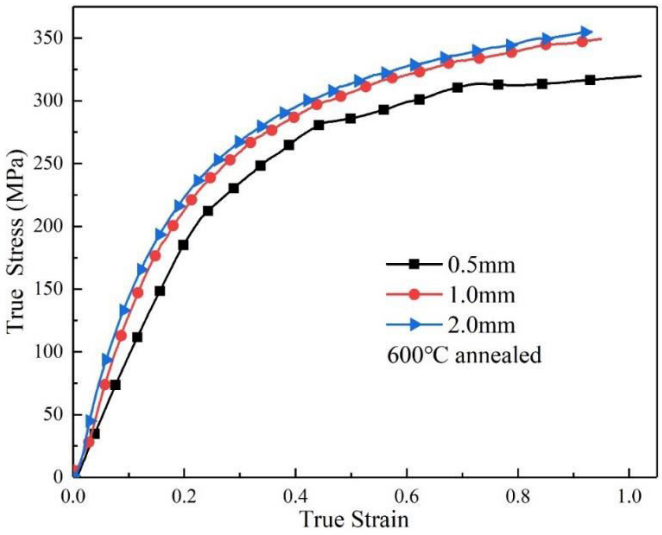

Fig.3. The true stress-strain curves of quasi-static compression for specimens with different geometrical sizes

3.2 SHPB experiments

As can be seen in Fig. 4, for the same geometrical and grain size, the flow stress of the specimen increase with increasing of strain rate, which shows a significant strain rate strengthening effect; and the degree of plastic deformation of the material increase with increasing of strain rate, which shows a strain rate induced plasticisation . This is inconsistent with the findings of most existing studies of macroscopic OFHC copper under dynamic loading, and there is uncertainty in strain rate sensitivity at macro-scale [24, 30, 31]. Zoller et al. [32] found that when the geometrical size was reduced, an increase in strain gradient led to an increase in dislocation density. According to Orowan's relationship, strain rate and stress are influenced by dislocation velocity and dislocation density [33, 34]. The strength of the material increases with increasing of dislocation density over a range of dislocation densities. When the sizes of the specimen reduce to micro/meso-scales, the strain gradient during the deformation under external dynamic loading lead to increasing of dislocation density. The increasing of dislocation density affects the dynamic mechanical properties of the specimen, which is why OFHC copper exhibits strain-rate strengthening effects at the micro/meso-scales. It can also be seen through Fig. 4 that there is some fluctuations in the dynamic true stress-strain curve of the specimen. At the micro/meso-scale, the surface grains are less constrained and the

deformation orientation of individual grains causes the non-uniformity of the plastic flow. The dynamic loading time is too short to coordinate the deformation between the grains, which leads to the fluctuations of the true stress.In Fig. 4 (b), the true stress-strain curve with a strain rate of 9000s^{-1} is significantly higher in the elastic stage and the initial stage of plastic deformation than the true stress-strain curve with a strain rate of 13000s^{-1}, possibly due to frictional effects and the instability of the air pressure during the experiments. As can be seen from Fig. 5, the flow stress of the specimens with the same grain size decreases as the decreasing of geometrical size under the same strain rate, which proves the phenomenon of ”the smaller, the weaker”. There was a slow growing stage in the true stress-strain curve of dynamic compression . In the dynamic compression process, the dynamic load response time is short and the energy generated by plastic deformation can not be released, which leads to the increasing of temperature in the specimen and the emergence of thermal softening effect. So the flow stress appears to have a slow growing stage.

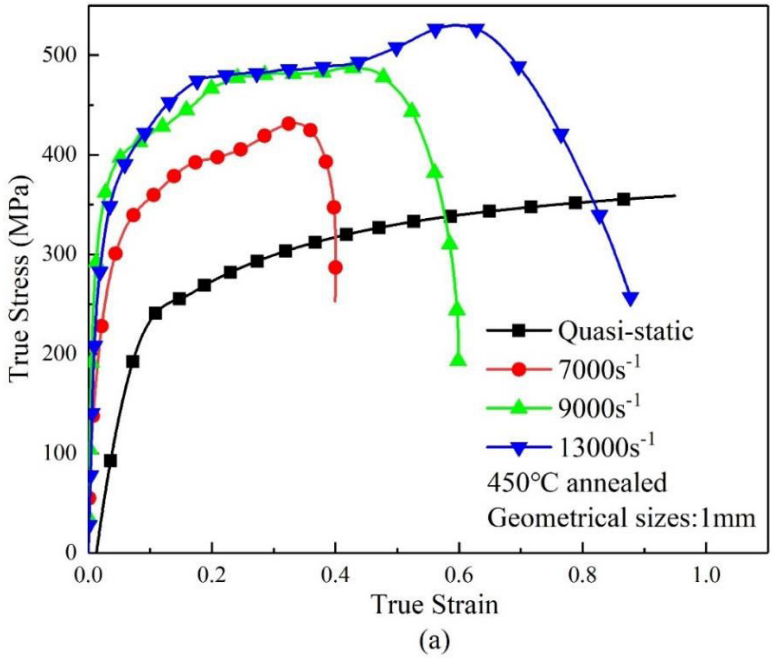

(a)

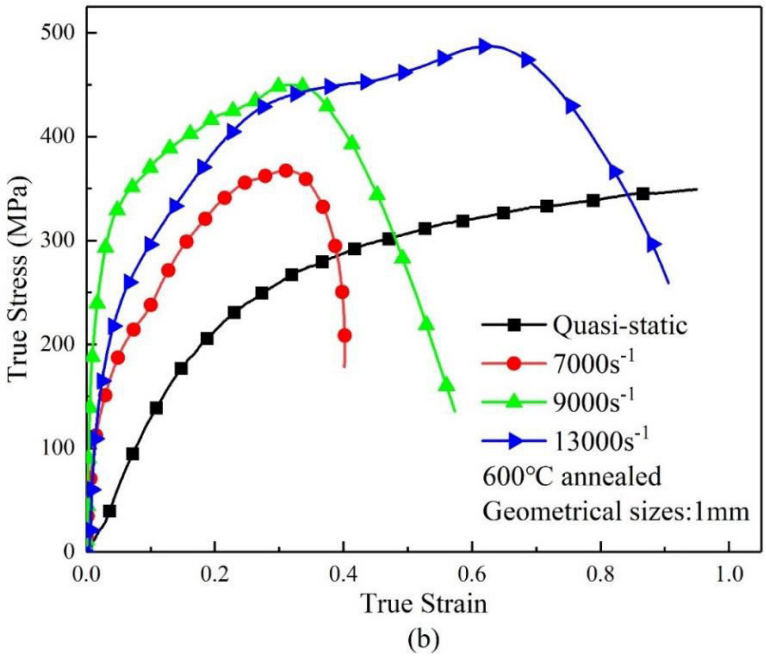

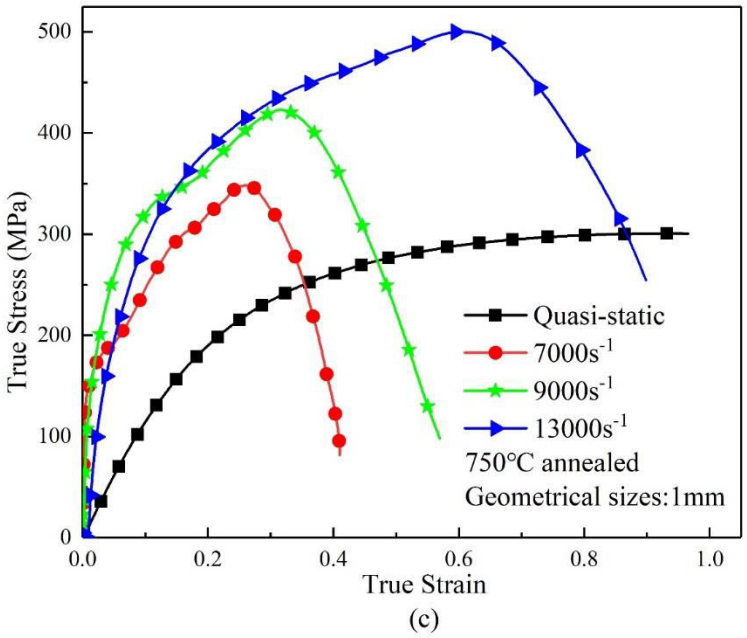

Fig.4. True stress-strain curves of dynamic compression for different specimens annealed at (a)450℃ , (b) 600℃ , and (c) 750℃ .

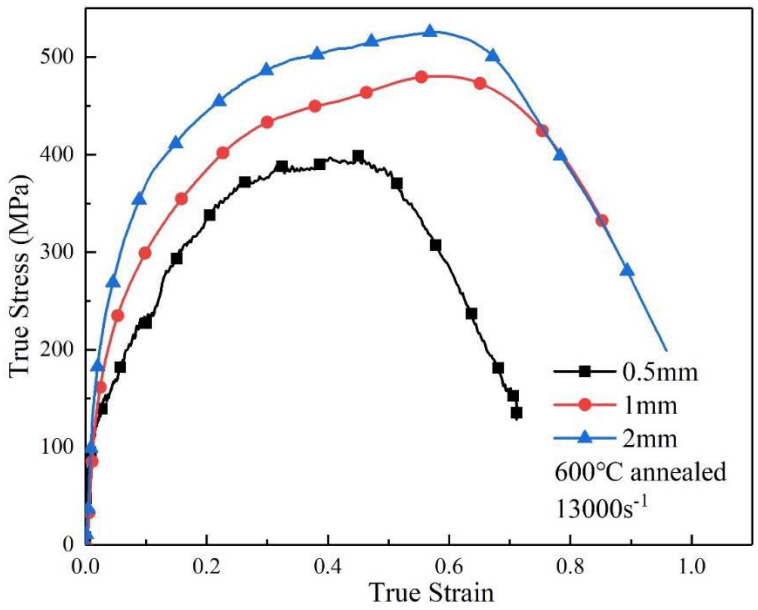

Fig.5. True stress-strain curves of dynamic compression for specimens with different geometrical sizes.

3.3 Metallographic and micro-morphological observations

The specimens were collected after the experiments, and then polished and etched to obtain metallographic photos, as shown in Fig. 6. The internal grains are compressed and elongated in the direction perpendicular to the direction of compression. After quasi-static and dynamic compression, the grains underwent elastic deformation and severe plastic deformation, the internal grains were compressed and elongated as shown in Fig. 6. Due to the short dynamic compression time and high impact velocity, the grains of the dynamically compressed specimens are flatter and more elongated than those of the quasi-statically compressed specimens, and even some grain boundaries are almost compressed together. Severe plastic deformation resulted in micro-cracks on the surface of the specimen in Fig.6 (a), which are not observed in the quasi-static compression specimen in Fig. 6 (b). The specimens after the quasi-static and dynamic compression experiments take the shape of a bulgen caused by friction, as shown by the dashed line in the Fig. 6. The flow direction of the circumferential surface grains is oriented at 45° to the direction of compression, as shown by the arrow in Fig. 6. At the micro/meso-scales, dynamic loading and random

grain distribution exacerbate the variation in grain orientation and inhomogeneous properties.

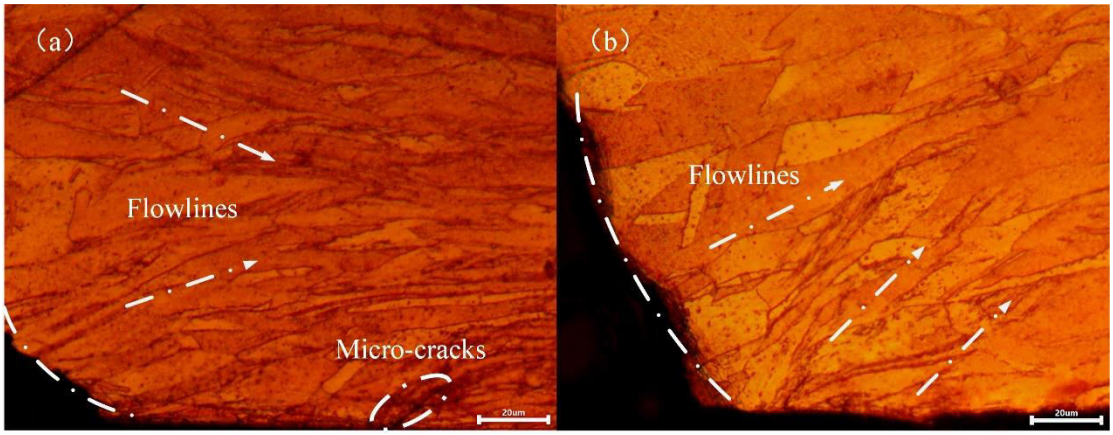

Fig. 6. Metallographic of post-experimental specimens, (a) SHPB and (b) quasi-static compression.

Fig. 7 shows the microscopic morphology of the quasi-static compression of the specimen of 1mm with different compression amount under the same heat treatment conditions. It can be seen that the specimen takes on a certain bulge shape during plastic deformation. The surface of the specimen becomes irregular as the degree of downward compression increases and micro-cracks begin to appear on the circumferential surface. When the degree of downward compression is 70%, the non-uniformity of grain flow on the surface of the specimen is greatest and the number of micro-cracks increases further. The microscopic morphology of specimens of different geometrical sizes with the same degree of compression are shown in Fig. 8. When the average grain size is equal and the degree of deformation is 50%, the unevenness of the specimen surface increases as the geometrical size decreases. This indicates the phenomenon of non-uniform flow of the specimen at the micro/meso-scales. The individual grain have different orientations so that each grain deforms differently when subjected to external forces. At the macro-scale, the grain size of the specimen is much smaller than the geometrical size and individual grain deformation can not affect the overall deformation, so that the specimen shows uniform deformation. On the one hand, the grain size and geometry of the specimen are on the same order of magnitude and the anisotropy of individual grains is not

negligible at the micro/meso-scales. The randomness of grain orientation leads to a non-uniformity in the plastic deformation process. On the other hand, the increasing of the ratio of surface grains to the overall grains makes the surface layer more susceptible to torsional deformation, which also leads to non-uniformity in the plastic deformation process.

The microscopic morphology of the specimens after the experiments with different heat treatment conditions and different strain rates are shown in Fig. 9. Under the same heat treatment conditions (in the same row), i.e. with the same average grain size, a shear slip zone is formed on the circumferential surface of the specimen at an angle of 45° to the direction of compression, and the degree of plastic deformation increases as the increasing of stress rate. For the same strain rate (in the same column), the shear slip on the specimen surface becomes more severe as the grain size increases.

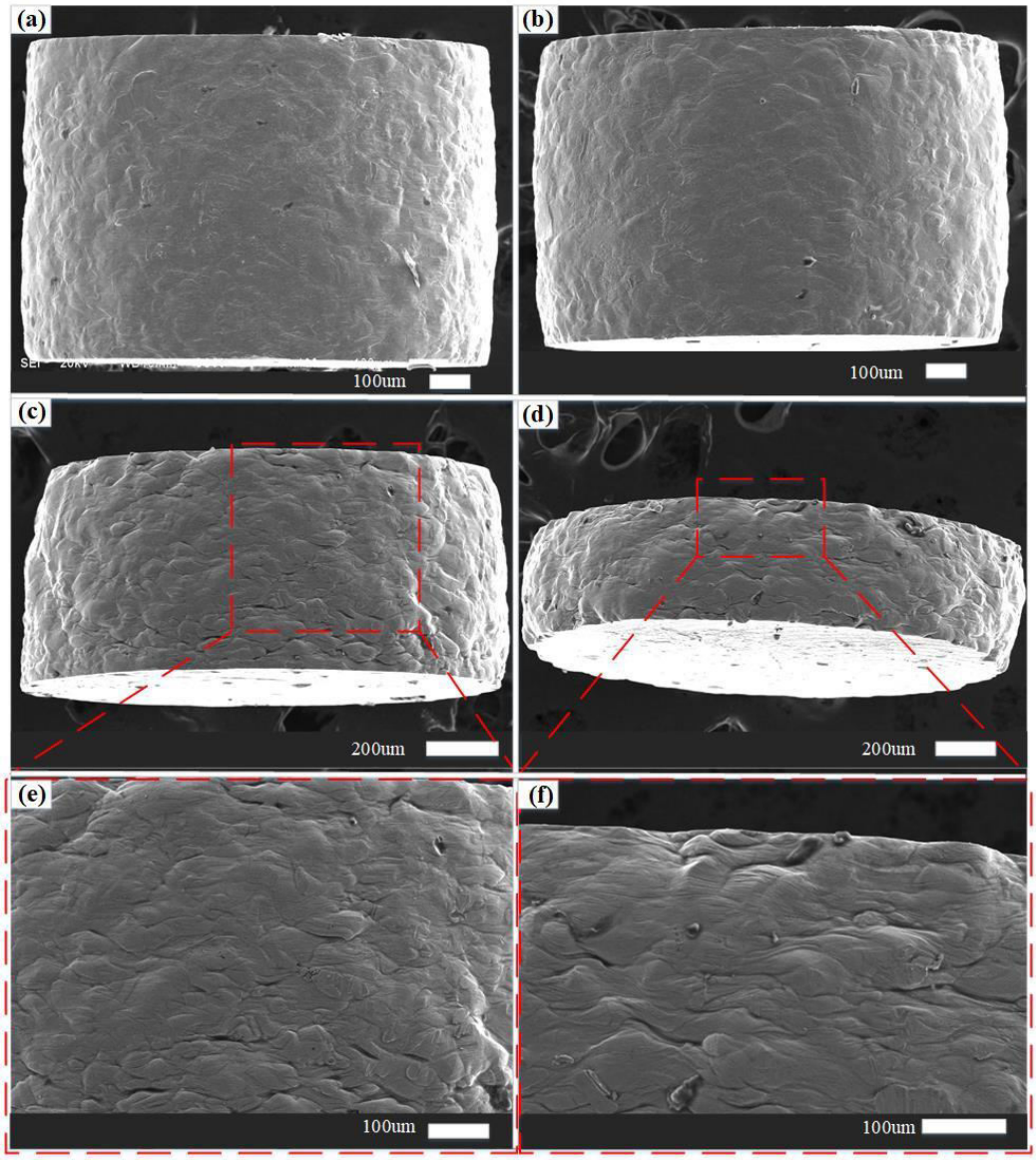

Fig. 7. Microscopic morphology of 1mm specimens with different degrees of deformation under the same heat treatment conditions.

(a) 30%, (b)40%, (c) 50%, and (d)70% .

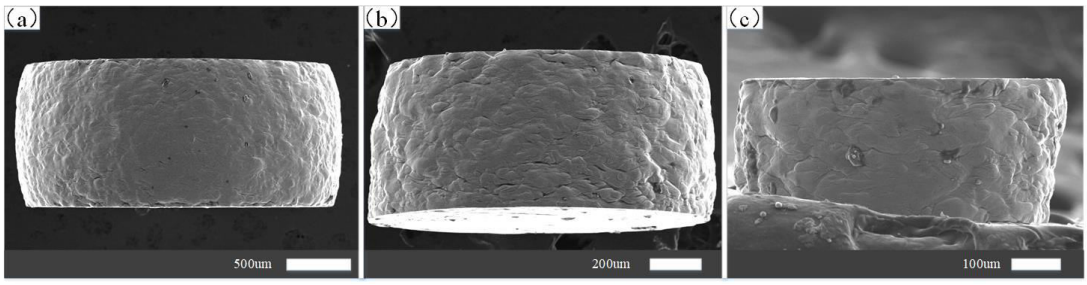

Fig. 8. Microscopic morphology of specimens of different geometrical sizeswith the same degree of deformation. (a) 2mm, (b)1mm, and (c)0.5mm.

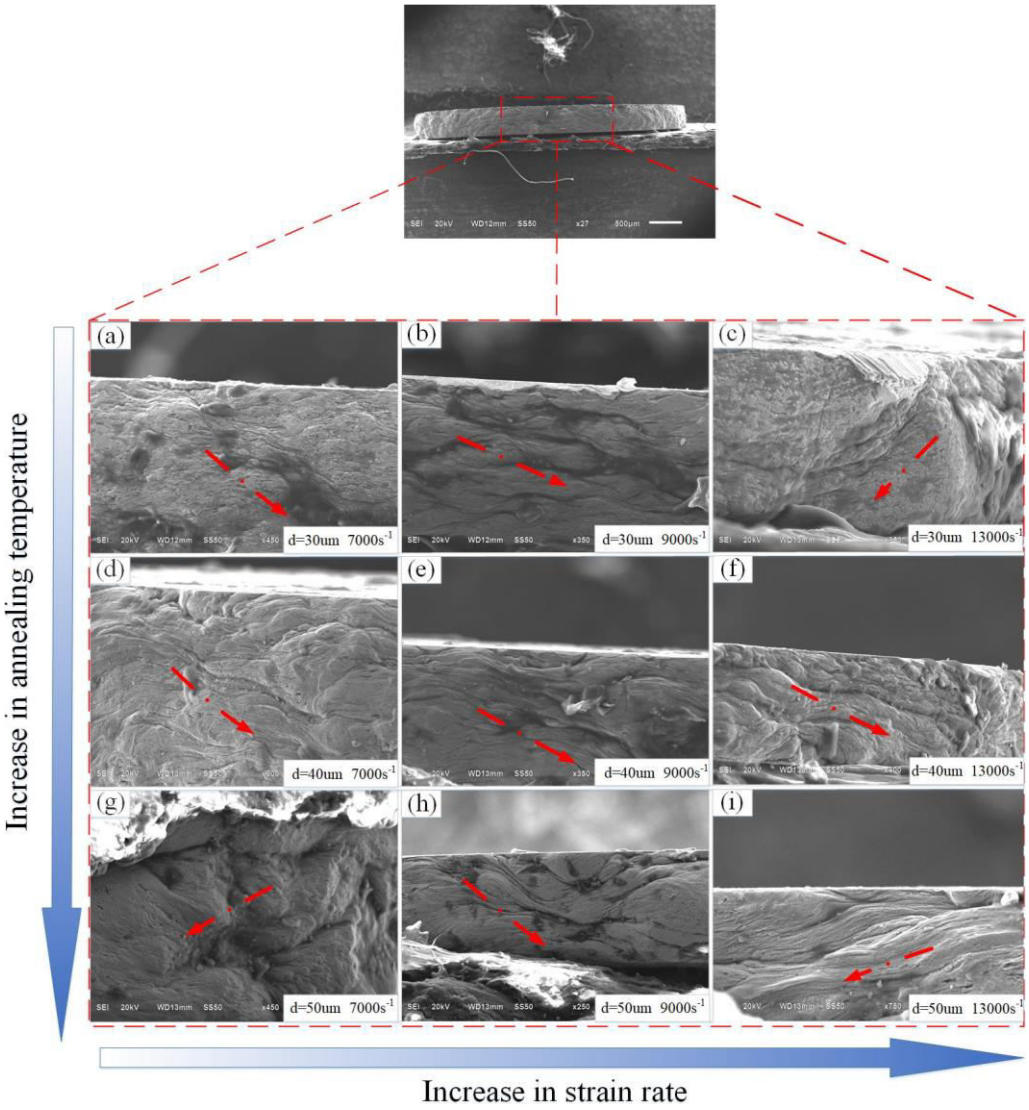

Fig.9. Microscopic morphology of specimens after experiments at different heat treatment temperatures and strain rates

3.4 The modified J-C constitutive equation based on surface layer model

3.3.1 Adiabatic temperature rise at high strain rates

The high-speed impact leads to a transient local temperature rise in the material, then cause a thermal softening effect of material. The equation for the adiabatic temperature rise of a material at high strain rates is

$$\Delta T = \frac{\beta}{\rho c_p} \int_0^{\bar{\varepsilon}_{pl}} \sigma_{ij} \, \mathrm{d}\varepsilon_{ij}^{pl} \tag{1}$$

Where ρ is the density of the material, and OFHC copper density is 8960kg/m^3, β

is the plastic work into the proportion of internal energy coefficient, generally taken as 0.9, c_p is the specific heat capacity of the material, taken as $390\,J/(\mathrm{kg}\cdot\mathrm{℃})$; $\int_0^{\bar{\varepsilon}_{pl}} \sigma_{ij}\,\mathrm{d}\varepsilon_{ij}^{pl}$ is the plastic deformation process of the work done by the flow of stress. Using the above equation, the adiabatic temperature rise can be calculated for 1mm specimens with different grain sizes and at different strain rates, as shown in Fig.10.

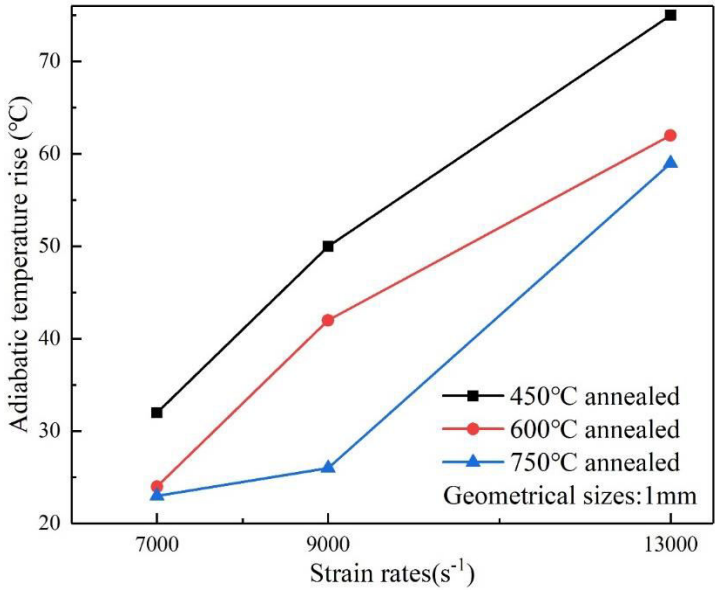

Fig.10. The adiabatic temperature rise of specimens with different grain sizes at different strain rates.

It can be seen from Fig.10 that the adiabatic temperature rise is increasingly obvious with the increasing of strain rate for the same grain size. The adiabatic temperature rise with the increasing of grain size for the same strain rate. The proportion of surface grains increases with the increasing of grain size, and the resistance of surface grains to deformation is lower than interior grains , then lower plastic work is converted to heat energy during deformation.

3.3.2 Surface layer model

As the geometrical size of the specimen decreases, the ratio of surface grains to all grains increases. It is known from crystal plasticity mechanics that the free surface cannot transfer and store dislocations, and the surface grains are less constrained and

more likely to twist and deform, which causes the flow stress to decrease as the size of specimen decreases during plastic deformation. The surface layer model considers the flow stress of the material to consist of the flow stress of surface grains and the internal grains, and the flow stress of the material can be written as:

$$\begin{cases} \sigma=\eta\sigma_{\mathrm{s}}+(1-\eta)\sigma_i \\ \eta=\dfrac{N_S}{N} \end{cases} \tag{2}$$

Where σ is the total flow stress, N is the total number of grains, N_s is the total number of surface grains, η is the ratio of surface grains to total grains, which is called the size factor, σ_{s} is the flow stress of superficial grains and σ_i is the flow stress of internal grains.

Base on the surface layer model, Lai et al. [35] proposed a hybrid intrinsic structure model that takes into account size effect. In this model, the surface grains are considered as a single crystal and the internal grains are considered as polycrystals. According to crystal plasticity theory and the Hall-Petch equation, the flow stresses in the surface and internal grains can be written as:

$$\begin{cases} \sigma_s(\varepsilon)=m\tau_R(\varepsilon) \\ \sigma_i(\varepsilon)=M\tau_R(\varepsilon)+\dfrac{k(\varepsilon)}{\sqrt{d}} \end{cases} \tag{3}$$

where d is the grain size, m and M are the orientation factors for single and polycrystalline grains respectively, $\tau_R(\varepsilon)$ is the principal decomposition shear stress of individual grains, and $k(\varepsilon)$ is the resistance stress at the grain boundary. Combining Eq. (2) and Eq. (3), the flow stress of the material at the micro/meso-scales can be written as:

$$\sigma(\bar{\varepsilon})=\eta m\tau_R(\bar{\varepsilon})+(1-\eta)\left(M\tau_R(\bar{\varepsilon})+\frac{k(\bar{\varepsilon})}{\sqrt{d}}\right) \tag{4}$$

When the ratio of surface grains to total grains is equal to zero, i.e. η=0, it means that

the geometry of the material is much larger than the grain size, and $\sigma(\bar{\varepsilon})$ represents a polycrystalline material model, when the ratio of surface grains to total grains is equal to one, i.e. η=1, it means that the geometry of the material is much equal to the grain size, and $\sigma(\bar{\varepsilon})$ represents a single crystal material model. Further simplification of Eq. (4) was given in [1]:

$$\begin{cases} \sigma(\bar{\varepsilon}) = \sigma_{ind} + \sigma_{dep} \\ \sigma_{ind} = M\tau_R(\bar{\varepsilon}) + \dfrac{k(\bar{\varepsilon})}{\sqrt{d}} \\ \sigma_{dep} = \eta\left(m\tau_R(\bar{\varepsilon}) - M\tau_R(\bar{\varepsilon}) - \dfrac{k(\bar{\varepsilon})}{\sqrt{d}} \right) \end{cases} \tag{5}$$

Where σ_{dep} is size-dependent flow stress and σ_{ind} is size-independent flow stress.

The specimens used in this study are cylinder and the relationship between the surface grains and the internal grains at the microscale is shown in Fig. 11. The diameter of the cylinder is D and the grain size is d. The volumes of the surface grains and the internal grains are as follows:

$$\begin{cases} \eta = \dfrac{N_S}{N} = \dfrac{\dfrac{\pi D^2 H}{4} - \left[\dfrac{\pi}{4}(D-2d)^2(H-2d)\right]}{\dfrac{\pi D^2 H}{4}} = 1 - \dfrac{\left[(D-2d)^2(H-2d)\right]}{D^2 H} & D \neq d \\ \eta = 1 & D = \mathrm{d} \end{cases} \tag{6}$$

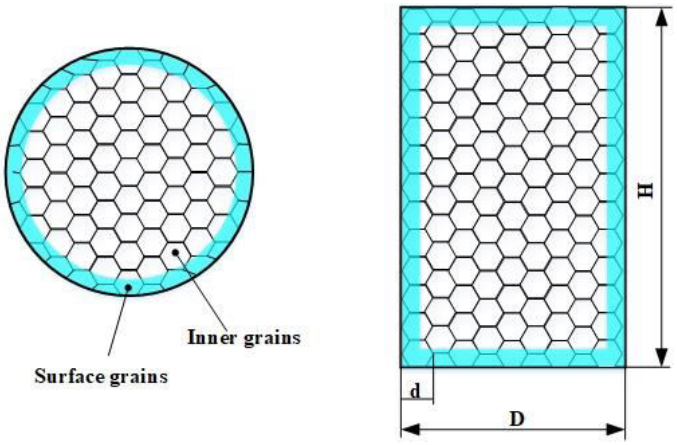

Fig.11 The surface layer model of the micro/meso-scales cylindrical sample.

3.3.3 The modified J-C model

The J-C model considers the flow stresses of metallic materials influenced by strain, strain rate, and temperature at deformation, and is widely used in the study of dynamic mechanics because of its simple form and easily available parameters. It can be written as:

$$\sigma = \left(A + B\varepsilon^{n}\right)\left(1 + C\ln\frac{\dot{\varepsilon}}{\dot{\varepsilon}_0}\right)\left[1 - \left(\frac{T - T_r}{T_m - T_r}\right)^{m}\right] \tag{7}$$

Where A is the initial yield stress of the material; B is the strain hardening coefficient; n is the hardening index; C is the strain rate strengthening coefficient; m is the thermal softening index; all of the above parameters can be obtained experimentally; ε is the equivalent plastic strain; $\dot{\varepsilon}_0$ is the reference strain rate; $\dot{\varepsilon}$ is the equivalent plastic strain rate; T is the actual temperature; T_r is the room temperature; T_m is the melting temperature.

According to the above study, the quasi-static and dynamic mechanical properties of the material are affected by size effects at the meso/micro-scales, so the size effects should be considered in the modified intrinsic structure model. Wang et al. [1] found that a hybrid damage model consisting of a surface layer model and the Hall-Petch equation was in good agreement with experimental results in predicting the quasi-static mechanical properties of materials at the micro/meso-scales. Therefore, the first term of the J-C model is replaced by a hybrid model. In this study, the strain-rate strengthening term is introduced to correct the term of strain rate in a similar form, taking into account the effect of size effects on dynamic mechanical properties. The modified J-C model can be written as:

$$\sigma = \left[M\tau_R(\varepsilon) + \frac{\mathrm{k}(\varepsilon)}{\sqrt{d}} + \eta\left(m\tau_R(\varepsilon) - M\tau_R(\varepsilon) - \frac{k(\varepsilon)}{\sqrt{d}} \right) \right] \left(1 + C\ln\frac{\dot{\varepsilon}}{\dot{\varepsilon}_0} \right)\left(1 + D\ln\frac{1}{\sqrt{\mathrm{d}}} \right)\left[1 - \left(\frac{T_W - T_r}{T_m - T_r} \right)^k \right] \tag{8}$$

$\tau_R(\varepsilon)$ and $\mathrm{k}(\varepsilon)$ can be viewed as exponential functions related to plastic strain and can be written as:

$$\begin{cases} \tau_R(\varepsilon) = k_1\varepsilon^{n_1} \\ k(\varepsilon) = k_2\varepsilon^{n_2} \end{cases} \tag{9}$$

In this study, the specimen with 1 mm was chosen to fit for the parameters of the constitutive equation, as several grain sizes and feature sizes were involved. In particular, the change in $\mathrm{k}(\varepsilon)$ was found to converge to a constant function in the parameter fitting, so $\mathrm{k}(\varepsilon)$ was set as a constant function. The fitted parameters of the original J-C and modified J-C are shown in Table 2 and Table 3.

Table 2. The fitted parameters of the original J-C

Annealed temp	A	B	C	n	m
450℃	178	199	0.04	0.36	
600℃	136	279	0.035	0.58	1.09
750℃	117	239	0.03	0.36	

Table 3. The fitted parameters of the modified J-C

Annealed temperature	m	M	k(ε)	n	η	C	D	k
450℃					0.116	0.028	-0.08	
600℃	168	235	29	0.26	0.168	0.013	-0.07	1.09
750℃					0.226	0.01	-0.045	

The comparison of the curves fitted by the original J-C model and the curves fitted by

the modified J-C model with the experimental results is shown in Fig. 12. It can be seen that the curves fitted by the original J-C model have large deviations from those obtained experimentally for different grain sizes and geometries, and cannot accurately reflect the dynamic mechanical properties of OFHC copper at the micro/meso-scales. The modified J-C model based on the surface layer model takes into account the effect of size effects on the dynamic mechanical properties of OFHC copper, and the curves fitted by the modified J-C model are in good agreement with the experimental results.

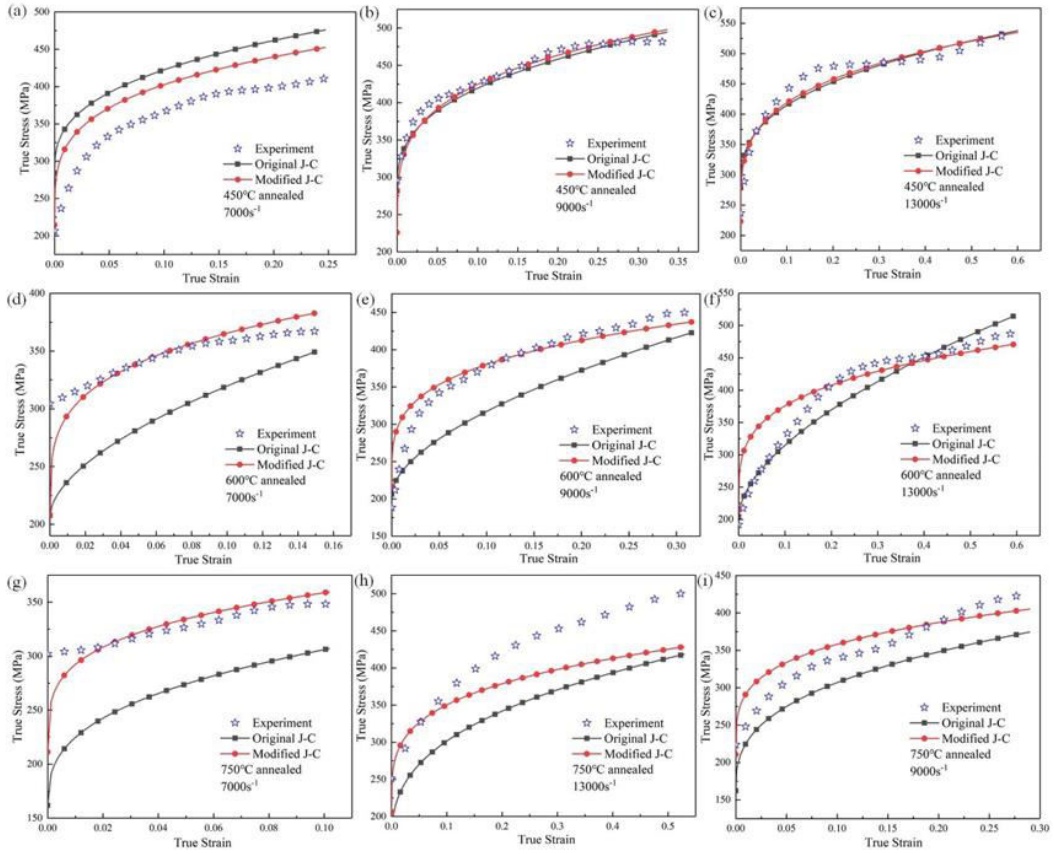

Fig.12. The comparison of the curves fitted by the original J-C model and those fitted by the modified J-C model with experimental results.

Using the average relative error $\overline{\delta}$ to analyze the experimental curve and fitted curve data, the relative error formula can be written as:

$$\overline{\delta} = \frac{1}{Z}\sum_{N=1}^{N}\left|\frac{E_i - P_i}{E_i}\right| \times 100\% \tag{10}$$

Where E_i is the experimental value, P_i is the fit value of the model, and Z is the total amount of data.

The relative error between the original J-Cmodel and the experimental results and the relative error between the modified J-C model and the experimental results are shown in Fig. 13. The average relative errors for the original J-C model ranged from 0.22% to 19% and the average relative errors for the modified J-C model ranged from 0.011% to 12%. The largest average relative error values for both the original J-C model and the modified J-C model fits occur at 450 °C for annealed specimens at a strain rate of 7000 s^{-1}. The accuracy of the modified J-C model is higher than the original J-C model except for the case of the 450 °C annealed specimen at a strain rate of 7000 s^{-1}. The mean of the average relative error of the original J-C model is 10.5 %, which is much higher than the mean of the average relative error of the modified J-C model which is 4.3 %. This indicates that the modified J-C model is more accurate in describing the dynamic mechanical properties of OFHC copper at micro/meso-scales.

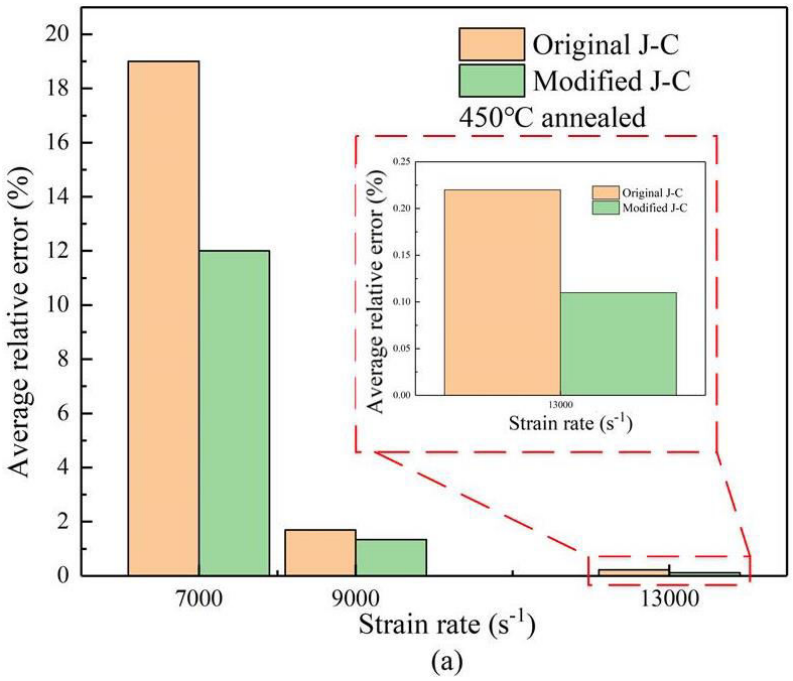

(a)

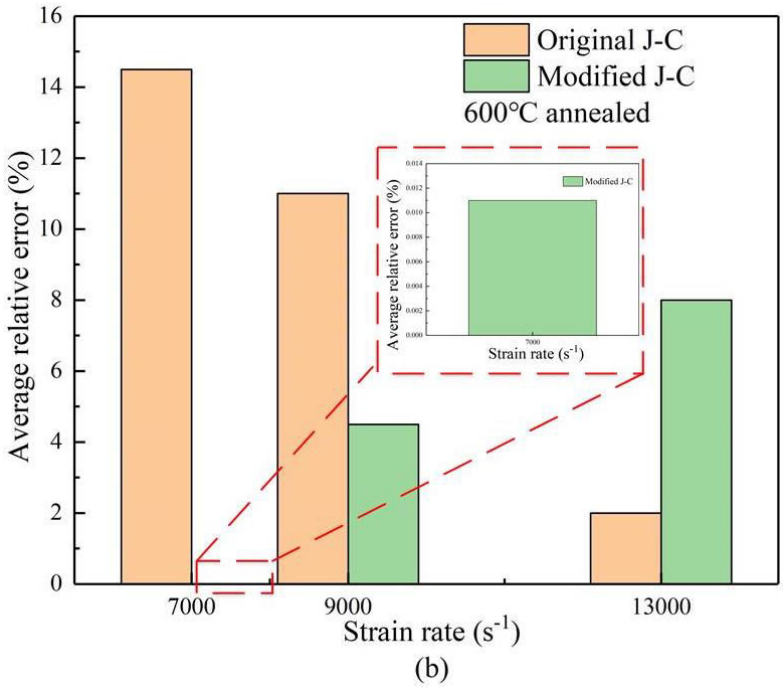

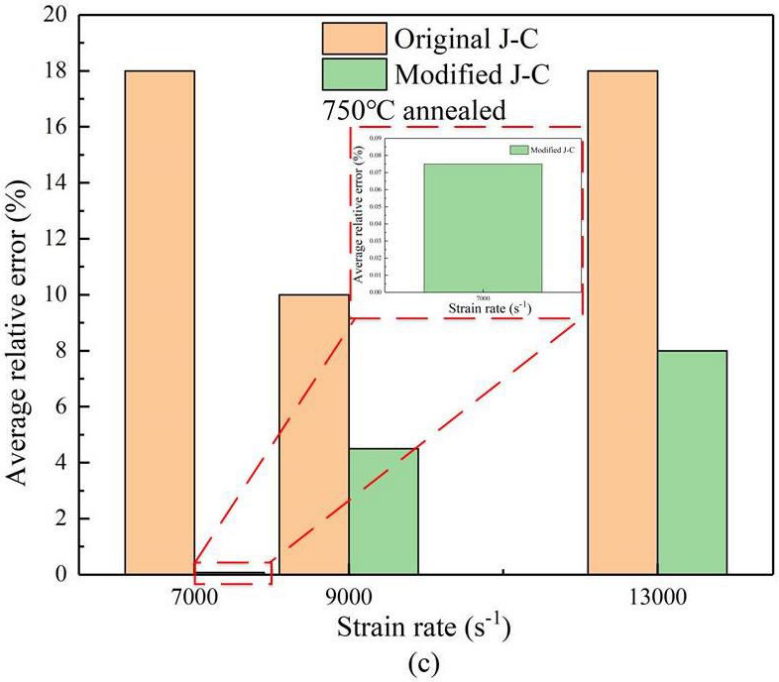

Fig.13. Relative error between the fitted values of the original and modified J-C models and the experimental data at different strain rates.

4. Numerical simulation

In this study, in order to verify the accuracy of the modified model, simulations were performed using ABAQUS, a commercial finite element simulation software with

powerful nonlinear computational capabilities. The dimensions of the incident rod, transmission rod, and specimen are the same as those used in the experiment. The material parameters of the original J-C model and the modified J-C model fitted in Section 3 are entered into the material properties in ABAQUS respectively. A certain velocity boundary condition is set for the free end of the incident rod in order to achieve the experimental effect of the impact rod hitting the incident rod in the test.

After FE simulation, the true stress-strain curves are obtained and show a significant size effect, as shown in Fig. 14. It can be seen that the original J-C model is significantly different from the experimental results in predicting the dynamic mechanical properties of OFHC copper at the micro/meso-scales. The numerical simulation results are lower than the experimental flow stress-strain and less accurate. This suggests that the presence of size effects at the micro/meso-scales affects the dynamic mechanical properties of the material and that the original J-C model is no longer suitable for predicting the dynamic mechanical properties of the material at the micro/meso-scales. The modified J-C model based on the surface layer model is in good agreement with the experimental results in predicting the mechanical properties at the micro/meso-scales, and the accuracy of the modified J-C model is much higher than that of the original J-C model. There are relatively more surface grains at the micro/meso-scales and the surface grains are less constrained leading to more prone to plastic deformation. The size effect on the dynamic mechanical properties of OFHC copper cannot be ignored, so taking the size factor into account in the constitutive model can significantly improve the accuracy of the model.

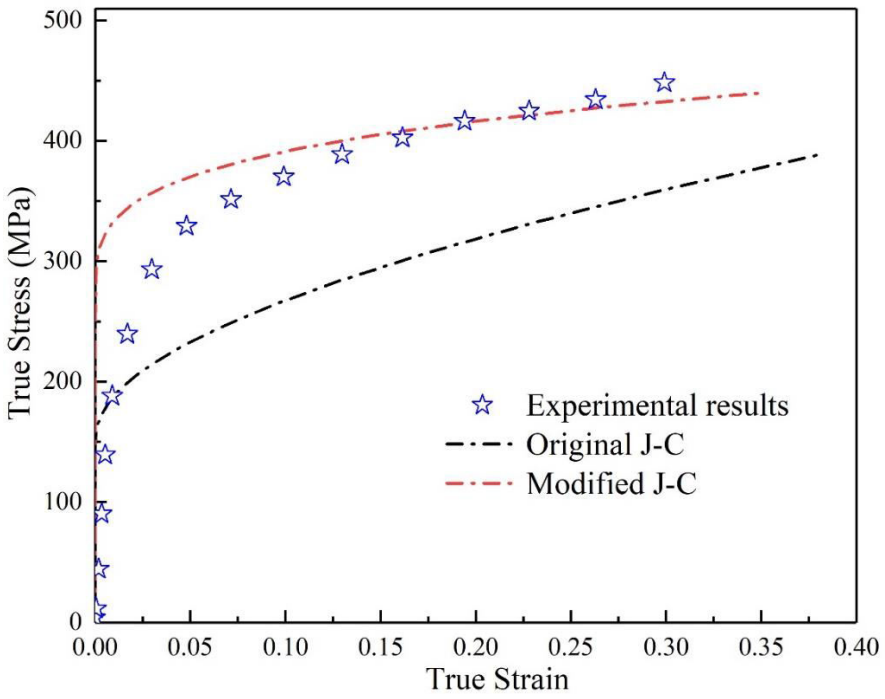

Fig.14. Comparison of the numerical simulation results of the original and modified J-C models with the experimental results.

5. Conclusion

In this study, the microstructure of OFHC copper with different grain sizes was obtained by heat treatment, and the influence of size effect on the quasi-static and dynamic mechanical properties of OFHC copper at the micro/meso-scales was investigated. Metallographic and micromorphological observations were made on the experimental specimens. A modified J-C model based on the surface layer model was proposed for predicting the dynamic mechanical properties of OFHC copper at the micro/meso-scale. The main conclusions of this thesis can be summarized as follows:

1. Both the quasi-static mechanical and dynamic mechanical properties of OFHC copper at the micro/meso-scales are influenced by the size effect. The grain size and geometrical size at the micro/meso-scales are on the same order of magnitude. The ratio of the surface grains to the total grains increases, i.e. η increases, as the surface grains are less constrained, the surface grains cannot store and transfer

dislocations and are more prone to plastic deformation.

2. The size effects on the mechanical properties of OFHC copper is more obvious at high strain rates. The dynamic loading times is transient and poor coordination of deformation between grains lead to deformation orientation of individual grains affecting the mechanical properties of the specimen. The degree of plastic deformation and the non-uniform flow in the specimens of SHPB is more severe than in the quasi-static specimens. The specimens of SHPB after the experiment also showed micro-cracks.

3. A modified J-C model based on the surface layer model was established. The experimental results were compared with the original and modified model and the average relative error analysis was performed. The results showed that the average relative errors for the original J-C model ranged from 0.22% to 19% and the average relative errors for the modified J-C model ranged from 0.011% to 12%.

4. The original and modified models were brought into ABAQUS for finite element simulation respectively, and the results of the numerical analysis indicate that the modified model has better agreement with the experimental results than the original J-C model.

Author contribution

Chuanzhi Jing was responsible for writing this papers and FE simulation.

The Corresponding author Jilai Wang was responsible for proposing methods and planning experiments.

Chengpeng Zhang and Zhenyu Shi were responsible for experiments and data collection.

Yan Sun was responsible for data processing and measuring working.

Funding

The authors gratefully acknowledge funding supported by the Young Scholars Program of Shandong University, Shandong Provincial Natural Science Foundation (ZR2019BEE062), China Postdoctoral Science Foundation (2021M691926), Natural Science Foundation of Jiangsu Province (BK20190202), Research Project of State Key Laboratory of Mechanical System and Vibration (MSV202102).

Data availability

Not applicable

Declarations

Ethical approval

Not applicable

Consent to participate

Not applicable

Consent to publish

Not applicable

Competing interests

The authors declare that they have no known competing financial interests or personal relationships that could have appeared to influence the work reported in this paper.

References

[1] J.L. Wang, M.W. Fu, S.Q. Shi (2017) Influences of size effect and stress condition on ductile fracture behavior in micro-scaled plastic deformation, Mater Design 131:69-80.

[2] J.Q. Ran, M.W. Fu, W.L. Chan (2013) The influence of size effect on the ductile fracture in micro-scaled plastic deformation, International Journal of Plasticity 41(1): 65-81.

[3] J.L. Wang, M.W. Fu, J.Q. Ran (2014) Analysis of size effect on flow-induced defect in micro-scaled forming process, International Journal of Advanced Manufacturing Technology 73(9-12) :1475-1484.

[4] M.W. Fu, J.L. Wang, A.M. Korsunsky (2016) A review of geometrical and microstructural size effects in micro-scale deformation processing of metallic alloy components, Int J Mach Tool Manu 109:94-125.

[5] M.W. Fu, J.L. Wang (2021) Size effects in multi-scale materials processing and manufacturing, Int J Mach Tool Manu 167: 103755.

[6] F. Jiang, L. Yan, Z.W. Hu, Y.M. Rong (2013) Size Effect Analysis during Material Deformation with High Strain Rate, Key Engineering Materials 589-590:198-203.

[7] D.-N. Zhang, Q.-Q. Shangguan, C.-J. Xie, F. Liu (2015) A modified Johnson–Cook model of dynamic tensile behaviors for 7075-T6 aluminum alloy, Journal of Alloys and Compounds 619:186-194.

[8] A.B. Tanner, R.D. McGinty, D.L. McDowell (1999) Modeling temperature and strain rate history effects in OFHC Cu, International Journal of Plasticity 15(6): 575-603.

[9] R. Smerd, S. Winkler, C. Salisbury, M. Worswick, D. Lloyd, M. Finn (2005) High strain rate tensile testing of automotive aluminum alloy sheet, Int J Impact Eng 32(1-4):541-560.

[10] L. Yang, P. Zhicong, L. Ming, W. Yonggang, W. Di, S. Changhui, L. Shuxin (2019) Investigation into the dynamic mechanical properties of selective laser melted Ti-6Al-4V alloy at high strain rate tensile loading, Materials Science and Engineering: A 745:440-449.

[11] P. Verleysen, J. Peirs (2017) Quasi-static and high strain rate fracture behaviour of Ti6Al4V, Int J Impact Eng 108:370-388.

[12] B.F. Wang, A. Fu, X.X. Huang, B. Liu, Y. Liu, Z.Z. Li, X. Zan (2016) Mechanical Properties and Microstructure of the CoCrFeMnNi High Entropy Alloy Under High Strain Rate Compression, Journal of Materials Engineering and Performance 25(7) :2985-2992.

[13] Z.N. Mao, X.H. An, X.Z. Liao, J.T. Wang (2018) Opposite grain size dependence of strain rate sensitivity of copper at low vs high strain rates, Mat Sci Eng a-Struct 738:430-438.

[14] W. Wang, M. Li, C. He, X. Wei, D. Wang, H. Du (2013) Experimental study on high strain rate behavior of high strength 600–1000MPa dual phase steels and 1200MPa fully martensitic steels, Mater Design 47:510-521.

[15] R.Q. Liang, A.S. Khan (1999) A critical review of experimental results and constitutive models for BCC and FCC metals over a wide range of strain rates and temperatures, International Journal of Plasticity 15(9): 963-980.

[16] G.R. Johnson, W.H. Cook (1985) Fracture characteristics of three metals subjected to various strains, strain rates, temperatures and pressures, Engineering Fracture Mechanics.

[17] A.S. Khan, S. Huang (1992) Experimental and theoretical study of mechanical behavior of 1100 aluminum in the strain rate range 10^{-5}–$10^{4}s^{-1}$, International Journal of Plasticity 8(4):397-424.

[18] B. Farrokh, A.S. Khan (2009) Grain size, strain rate, and temperature dependence of flow stress in ultra-fine grained and nanocrystalline Cu and Al: Synthesis, experiment, and constitutive modeling, International Journal of Plasticity 25(5):715-732.

[19] A. Molinari, G. Ravichandran (2005) Constitutive modeling of high-strain-rate deformation in metals based on the evolution of an effective microstructural length, Mechanics of Materials 37(7):737-752.
[20] H. Shi, A.J. McLaren, C.M. Sellars, R. Shahani, R. Bolingbroke (1997) Constitutive equations for high temperature flow stress of aluminium alloys, Materials Science and Technology 13(3):210-216.
[21] F.J. Zerilli, R.W. Armstrong (1987) Dislocation-Mechanics-Based Constitutive Relations for Material Dynamics Calculations, J Appl Phys 61(5):1816-1825.
[22] P.S. Follansbee, U.F. Kocks (1988) A Constitutive Description of the Deformation of Copper Based on the Use of the Mechanical Threshold Stress as an Internal State Variable, Acta Metall Mater 36(1):81-93.
[23] S. Nemat-Nasser, J.B. Isaacs (1997) Direct measurement of isothermal flow stress of metals at elevated temperatures and high strain rates with application to Ta and TaW alloys, Acta Materialia 45(3): 907-919.
[24] H. Huh, K. Ahn, J.H. Lim, H.W. Kim, L.J. Park (2014) Evaluation of dynamic hardening models for BCC, FCC, and HCP metals at a wide range of strain rates, Journal of Materials Processing Technology 214(7):1326-1340.
[25] H.K. Farahani, M. Ketabchi, S. Zangeneh (2017) Determination of Johnson–Cook Plasticity Model Parameters for Inconel718, Journal of Materials Engineering and Performance 26(11):5284-5293.
[26] F. Ducobu, E. Riviere-Lorphevre, E. Filippi (2017) On the importance of the choice of the parameters of the Johnson-Cook constitutive model and their influence on the results of a Ti6Al4V orthogonal cutting model, International Journal of Mechanical Sciences 122:143-155.
[27] L. Gambirasio, E. Rizzi (2016) An enhanced Johnson–Cook strength model for splitting strain rate and temperature effects on lower yield stress and plastic flow, Computational Materials Science 113: 231-265.
[28] W.L. Chan, M.W. Fu, J. Lu, J.G. Liu (2010) Modeling of grain size effect on micro deformation behavior in micro-forming of pure copper, Mat Sci Eng a-Struct 527(24-25): 6638-6648.
[29] W.L. Chan, M.W. Fu, J. Lu (2011) The size effect on micro deformation behaviour in micro-scale plastic deformation, Mater Design 32(1):198-206.
[30] B. Zhang, V.P.W. Shim (2010) Determination of inelastic heat fraction of OFHC copper through dynamic compression, Int J Impact Eng 37(1):50-68.
[31] J.L. Jordan, C.R. Siviour, G. Sunny, C. Bramlette, J.E. Spowart (2013) Strain rate-dependant mechanical properties of OFHC copper, J Mater Sci 48(20):7134-7141.
[32] K. Zoller, K. Schulz (2020) Analysis of single crystalline microwires under torsion using a dislocation-based continuum formulation, Acta Materialia 191:198-210.
[33] H.D. Fan, Q.Y. Wang, J.A. El-Awady, D. Raabe, M. Zaiser (2021) Strain rate dependency of dislocation plasticity, Nature Communications 12(1):1-11.
[34] Q. Kun, Y. Li-Ming, H. Shi-Sheng (2009) Mechanism of Strain Rate Effect Based on Dislocation Theory, Chinese Physics Letters 26(3):036103.
[35] X.M. Lai, L.F. Peng, P. Hu, S.H. Lan, J. Ni (2008) Material behavior modelling in micro/meso-scale forming process with considering size/scale effects, Computational Materials Science 43(4):1003-1009.